# A Mathematical Characterization and Analysis of a Feedforward Circuit for CDMA Applications

A. Hakan Coskun, *Student Member, IEEE,* and Simsek Demir, *Member, IEEE*

***Abstract*—Feedforward is known to be one of the best methods for power amplifier linearization due to its superior linearization performance albeit with relatively poor power efficiency. Here we present the derived closed-form expressions, which relate the main channel power and distortion products at the output of a simple feedforward circuitry to the circuit parameters. Consequently, a mathematical handy tool is achieved toward specifying the circuit parameters rapidly for optimum linearity performance and efficiency. The main and error amplifiers used in the feedforward are assumed to have a third-order AM/AM nonlinearity. The derived expressions are verified by simulation. The conditions for the validity of the model choice are highlighted. For the matched and lossless case, a compact relationship is obtained, which clearly demonstrates the tradeoff between nonlinearities of main and error amplifier for a given system linearity and output power. Delay mismatch is also included in the analysis.**

***Index Terms*—Band-limited white Gaussian noise, CDMA, feedforward, linearization, peak-to-average ratio, stochastic characterization.**

## I. Introduction

TODAY, most modern communication systems use digital modulation such as QPSK and QAM. Hence, it is possible to transmit more data at high data rates and preserve the quality of the signal without loss of information. In cellular communication systems, digital modulation schemes where the information is carried are accessed by various systems such as time division multiple access (TDMA) and code division multiple access (CDMA). In CDMA systems, a certain number of users can communicate at the same time and frequency as long as each user uses a unique code. This makes CDMA spectrally efficient and popular in modern communication systems. However, the resulting signal has a high envelope peak-to-average ratio (crest factor) and linear power amplifiers with high back-off are required in order not to degrade the quality of the signal. Linear power amplifiers that have high back-off power and high IP3 give rise to the problem of efficiency. In order to increase the linearity performance of the system, various linearization techniques such as predistortion, envelope elimination and restoration, Cartesian feedback, and feedforward are used [1], [2]. Among these methods, feedforward has a better linearization performance and provides a more broad-band stable operation since there is no feedback path whereas it has the limitation of efficiency [3].

A typical feedforward system involves two cancellation loops [3]. The first one is the carrier cancellation loop, which extracts the distortion products, and the second one is the error cancellation loop, which amplifies the distortion products and eliminates them by canceling with the distorted main amplifier output. The amplifier used in this loop is called the error amplifier and it must be sufficiently linear in order not to introduce extra distortion products. Since feedforward is based upon the cancellation of nearly equal amplitude signals, the distortion signal at the input of the error amplifier usually has a very high envelope peak-to-average ratio (typically much more than that of the main amplifier input or output) which requires the error amplifier to have a high IP3 although the average power is at a moderate level if the carrier cancellation is good. Amplitude, phase, and delay mismatches are the main constraints on the linearization performance of the feedforward, and its efficiency is limited by the IP3 of the main and error amplifiers, losses of the couplers, and delay compensators.

In [4], closed-form expressions for the linearity performance of a memoryless CDMA RF power amplifier whose third- and fifth-order nonlinearities are specified by IP3 and IP5 parameters have been derived. Such an expression gives the designer a tool to determine the necessary IP3 of the power amplifier for a given linearity requirement. For a complete feedforward system where two power amplifiers and couplers participate, a similar closed-form expression, which relates the linearity performance to the parameters of the whole linearizer and signal characteristics may be required. Using such a tool, system parameters can be optimized for optimum efficiency and given linearity performance. A closed-form expression for a feedforward circuit, which formulates the output main channel power and adjacent channel power (ACP) for CDMA applications has not been derived yet.

In this paper, the approach used in [4] is extended to a simple feedforward circuitry for a typical CDMA application. For the sake of simplicity, in the beginning no delay and phase mismatch is assumed, and the main and error amplifiers used in the system are considered to have a third-order AM/AM nonlinearity only. First, the transfer function of the feedforward circuit shown in Fig. 1 will be derived. Then using this transfer function, closed-form expressions, which characterize the main amplifier and feedforward output will be derived by making use of the stochastic characterization of the input CDMA signal. The derived closed-form expressions are then verified through simulations.

Manuscript received November 30, 2001; revised October 9, 2002.

A. H. Coskun is with the Communications Division, ASELSAN Electronics Industries Inc., Ankara, Turkey.

S. Demir is with the Department of Electrical and Electronics Engineering, Middle East Technical University, Ankara, Turkey.

Digital Object Identifier 10.1109/TMTT.2003.808582

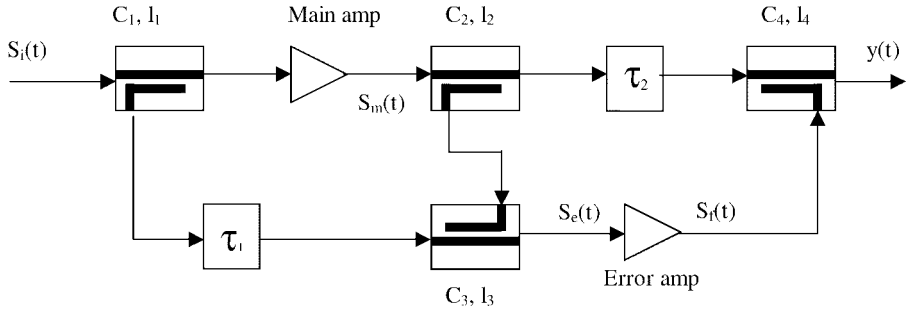


Fig. 1. Simplified form of a feedforward circuit.

As a consequence of these derivations, closed-form expressions, which provide a tool to control circuit parameters for optimum efficiency and linearity and to compute main channel power and ACP easily, are obtained. The conditions for the validity of these expressions are brought into consideration. Then, for a special case, we end up with a compact relationship, which clearly demonstrates the tradeoff between main and error amplifier nonlinearities. Finally, the derived closed-form expressions are modified to demonstrate the effect of the delay mismatch in the second loop. On the other hand, the delay mismatch in the first loop has not been included in the content of the paper because the resultant expressions are lengthy due to the transformation of delay mismatches through the error amplifier. As the last step, to bring the usefulness of third-order modeling into consideration, simulation results are generated and compared for third- and fifth-order amplifier models.

## II. Transfer Function of a Feedforward Circuit

A simplified feedforward circuit is illustrated in Fig. 1. Input signal to the feedforward circuit can be expressed as follows:

$$s(t) = s_i(t)\cos(2\pi f_c t + \theta(t)) \tag{1}$$

where $s_i(t)$ is the envelope of the input signal and $f_c$ is the carrier frequency. Since the main amplifier is assumed to be memoryless, the output of the main amplifier can be expressed by the following power series expansion:

$$s'_{mo}(t) = l_1 a'_1 s(t) + l_1^3 a'_3 s^3(t) \tag{2}$$

where $l_1$ is the loss of the coupler C1 and $a'_1$ and $a'_3$ are the power series coefficients which characterize the third-order nonlinearity of the main amplifier and they can be written in terms of the gain $G_m$ (dB) and $\mathrm{IP}_3^m$ (dBW) of the amplifier [5] as

$$a'_1 = 10^{G_m/20} \quad a'_3 = \frac{-2}{3R}\,10^{((-\mathrm{IP}_3^m/10)+(3G_m/20))}. \tag{3}$$

Note that $R$ is the reference impedance of the circuit, which is usually 50 $\Omega$. Substituting (1) and neglecting third-order harmonics, (2) can be expressed as follows:

$$s_{mo}(t) = s_m(t)\cos(2\pi f_c t + \theta(t)) \tag{4}$$

where

$$s_m(t) = l_1 a_1 s_i(t) + l_1^3 a_3 s_i^3(t) \tag{5}$$

$$a_1 = a'_1$$
$$a_3 = \frac{3}{4}a'_3 \tag{6}$$

since

$$\cos^3(\theta) = \frac{3}{4}\cos(\theta) + \frac{1}{4}\cos(3\theta). \tag{7}$$

It should be recalled that third-order harmonics are neglected since they are outside the scope of analysis. The envelope of the signal at the input of the error amplifier can be expressed as follows, assuming there is no phase mismatch:

$$s_e(t) = \frac{s_m(t)}{C_2 C_3} - \frac{l_3 s_i(t)}{C_1} \tag{8}$$

where $C_1$, $C_2$, and $C_3$ are the coupling coefficients of the couplers C1, C2, and C3, respectively, and $l_3$ is the loss factor of C3. Envelope of the output of the error amplifier is

$$s_f(t) = b_1 s_e(t) + b_3 s_e^3(t) \tag{9}$$

where

$$b_1 = b'_1 \quad b_3 = \frac{3}{4}b'_3. \tag{10}$$

Note that $b'_1$ and $b'_3$ are Taylor series coefficients of the error amplifier, which has a third-order nonlinearity, and (3) is also valid for these coefficients. Finally, the envelope of the error cancellation loop output (feedforward output) can be written as

$$y(t) = l_2 l_4 s_m(t) - \frac{s_f(t)}{C_4} \tag{11}$$

where $l_4$ and $C_4$ are the loss factor and coupling coefficient of the coupler C4, respectively. If we combine the above equations and rearrange terms, we obtain the following simplified result:

$$y(t) = D_1 s_i(t) + D_3 s_i^3(t) + D_5 s_i^5(t) + D_7 s_i^7(t) + D_9 s_i^9(t) \tag{12}$$

where the coefficients can be found in Appendix A. To show the utility of (12), $y(t)$ versus $s_i(t)$ has been plotted for various $\mathrm{IP3}^e$

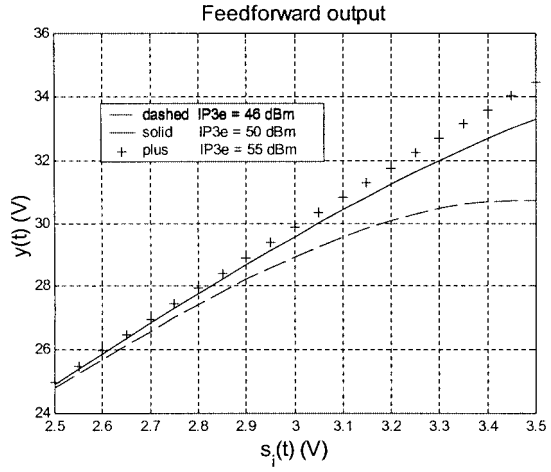


(a)

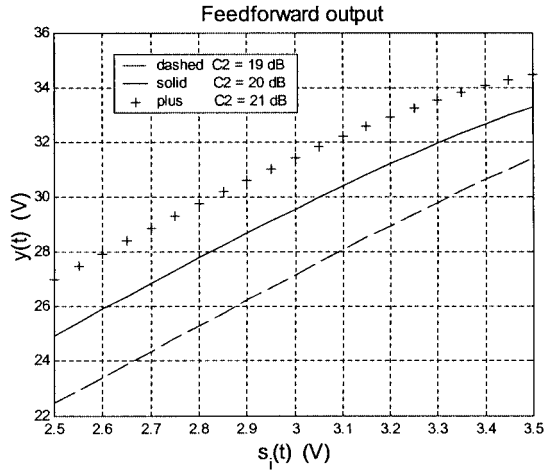


(b)

Fig. 2. (a) Response of (12) for various $\mathrm{IP3}^e$ values ($\mathrm{IP3}^m = 45.5$ dBm, $Gm = 20$ dB, $Ge = 40$ dB, $C_1 = C_3 = C_4 = 10$ dB, $C_2 = 20$ dB). (b) Response of (12) for various $C_2$ values ($\mathrm{IP3}^m = 45.5$ dBm, $Gm = 20$ dB, $\mathrm{IP3}^e = 50$ dBm, $Ge = 40$ dB, $C_1 = C_3 = C_4 = 10$ dB).

(error amplifier IP3 which is related to $b_1$ and $b_3$) and $C_2$ values in Fig. 2. It should be noted that $s_i(t)$ and $y(t)$ correspond to instantaneous feedforward input and output envelope voltages at the fundamental frequency, respectively.

## III. Main Amplifier and Feedforward Output Characterization

In order to derive a closed-form expression for power spectrum of the signal at the output of the feedforward circuit using the transfer function derived above, we have to characterize the input signal. If we can define the stochastic characterization of the input signal such as its probability density function (pdf), power histogram, autocorrelation function (AF), or power spectral density (PSD) explicitly, then we can find out the AF and PSD at any point in the feedforward circuit. Hence, we can derive a closed-form relationship between the ACP and the circuit parameters such as coupling coefficients, main and error amplifier gain, and IP3s. In our analysis, the input is a CDMA with $n$ spread spectrum signals. A general CDMA signal can be expressed as follows [6]:

$$s(t) = \sum_{i=1}^{n} m_i(t) c_i(t) \cos[2\pi f_c t + \theta_i(t)] \tag{13}$$

where $m_i(t)$ is the $i$th baseband modulated signal, $c_i(t)$ is the $i$th pseudonoise binary code whose bandwidth is $B$ which determines the bandwidth of the main channel, and $f_c$ is the carrier frequency. According to the law of large numbers and the central limit theorem, as the number of spread spectrum signals $n$ becomes larger, the overall signal $s(t)$ converges to a band-limited white Gaussian noise with zero mean [4], [6]. Such a signal has a well-known AF and PSD. Hence, (13) can be written as

$$s(t) = s_i(t) \cos[2\pi f_c t + \theta(t)] \tag{14}$$

where $s_i(t)$ is a Gaussian wide-sense stationary process with PSD

$$P_s(f) = \begin{cases} \dfrac{N_0}{2}, & |f| \le B \\ 0, & \text{else} \end{cases} \tag{15}$$

and with AF

$$R_{si}(\tau) = E\{s_i(t) s_i(t+\tau)\} = \frac{N_0 \sin(2\pi B\tau)}{2\pi\tau} \tag{16}$$

where $E\{\bullet\}$ denotes the expected value and $N_0$ is equal to $kT_e$ where $k$ is the Boltzmann's constant and $T_e$ is the equivalent noise temperature [7]. Our first step is to determine the AF for the main amplifier and feedforward output. Hence, by using (5), the AF for the envelope of the main amplifier output can be written as follows:

$$\begin{aligned} R_{sm}(\tau) &= E\{s_m(t) s_m(t+\tau)\} \\ &= E\{[E_1 s_i(t) + E_3 s_i^3(t)][E_1 s_i(t+\tau) + E_3 s_i^3(t+\tau)]\} \end{aligned} \tag{17}$$

where

$$E_1 = a_1 l_1 \quad E_3 = a_3 l_1^3. \tag{18}$$

For a Gaussian process with zero mean, (17) can be expanded and simplified as follows:

$$R_{sm}(\tau) = N_1 R_{si}(\tau) + N_3 R_{si}^3(\tau) \tag{19}$$

where

$$N_1 = E_1^2 + 9E_3^2 K^2 + 6E_1 E_3 K \tag{20}$$

$$N_3 = 6E_3^2 \tag{21}$$

$$K = N_0 B. \tag{22}$$

Similarly, the feedforward output AF can be derived as follows:

$$\begin{aligned} R_y(\tau) &= E\{y(t)y(t+\tau)\} \\ &= M_1 R_{si}(\tau) + M_3 R_{si}^3(\tau) + M_5 R_{si}^5(\tau) + M_7 R_{si}^7(\tau) \\ &\quad + M_9 R_{si}^9(\tau). \end{aligned} \tag{23}$$

Coefficients indicated in (23) are explicitly found in Appendix B and can be computed using the following closed-form expression which can be derived for a zero-mean wide-sense stationary Gaussian process by differentiating the joint characteristic function of two jointly Gaussian random variables

$$\begin{aligned} &E\{s^m(t)s^n(t+\tau)\} \\ &= 1\cdot 3\cdots n \cdot \sum_{k=1,3,5}^{m} R_s^k(\tau) K^{((m+n)/2)-k} \cdot \prod_{j=1,3}^{m-k-1} j \\ &\quad \cdot \prod_{j=1,3}^{k-2} (n-j) \cdot \binom{m}{k}, \qquad \text{for } m \le n,\ m,\ n \text{ odd}. \end{aligned} \tag{24}$$

Once the AF of the envelopes of the main amplifier and feedforward output are determined, PSD functions can be found by taking the Fourier transform of the AFs. The PSD of the signals at the output of the main amplifier and feedforward output are given by

$$P_m(f) = N_1 P_s(f) + N_3 P_s(f) \otimes P_s(f) \otimes P_s(f) \tag{25}$$

$$\begin{aligned} P_y(f) &= M_1 P_s(f) + M_3 P_s(f) \otimes P_s(f) \otimes P_s(f) \\ &\quad + M_5 P_s(f) \otimes P_s(f) \otimes P_s(f) \otimes P_s(f) \otimes P_s(f) \\ &\quad + M_7 P_s(f) \otimes \cdots \otimes P_s(f) \end{aligned} \tag{26}$$

where $\otimes$ denotes convolution. Note that up to seventh-order coefficients are taken into consideration while computing the third-order distortion products. The ninth-order has been observed to be negligible. In our analysis, the parameter $K = N_0 B$ is replaced by the following expression:

$$K = \frac{2P_m}{a_1^2 l_1^2} \tag{27}$$

where $K/2$ is the main channel input power and $P_m$ is the linear output power of the main amplifier if there were no in-band distortion. After expanding (25) and (26), closed-form expressions for PSDs have been derived as follows:

$$P_m(f) = \begin{cases} N_3 \left(\frac{N_0}{2}\right)^3 \left[\frac{f^2}{2} + 3Bf + \frac{9}{2}B^2\right], \\ \quad -3B < f < -B \\ N_1 \frac{N_0}{2} + N_3 \left(\frac{N_0}{2}\right)^3 [-f^2 + 3B^2], \\ \quad -B < f < B \\ N_3 \left(\frac{N_0}{2}\right)^3 \left[\frac{f^2}{2} - 3Bf + \frac{9}{2}B^2\right], \\ \quad B < f < 3B \end{cases} \tag{28}$$

and

$$P_y(f) = \begin{cases} M_3 \left(\frac{N_0}{2}\right)^3 \left[\frac{f^2}{2} + 3Bf + \frac{9}{2}B^2\right] + M_5 \left(\frac{N_0}{2}\right)^5 \\ \quad \left[\frac{-f^4}{6} - \frac{5}{3}Bf^3 - 5B^2f^2 - \frac{5}{3}B^3f + \frac{55}{6}B^4\right] \\ \quad + M_7 \left(\frac{N_0}{2}\right)^7 \left[\frac{15}{720}f^6 + \frac{35}{120}Bf^5 + \frac{63}{48}B^2f^4 \right. \\ \qquad \left. + \frac{35}{36}B^3f^3 - \frac{273}{48}B^4f^2 + \frac{35}{120}B^5f \right. \\ \qquad \left. + \frac{23\,583}{720}B^6\right], \qquad -3B < f < -B \\ M_1 \frac{N_0}{2} + M_3 \left(\frac{N_0}{2}\right)^3 \left[-f^2 + 3B^2\right] \\ \quad + M_5 \left(\frac{N_0}{2}\right)^5 \left[\frac{f^4}{4} - \frac{5}{2}B^2f^2 + \frac{230}{24}B^4\right] + M_7 \left(\frac{N_0}{2}\right)^7 \\ \quad \cdot \left[\frac{-20}{720}f^6 + \frac{28}{48}B^2f^4 - \frac{308}{48}B^4f^2 + \frac{23\,548}{720}B^6\right], \\ \qquad -B < f < B \\ M_3 \left(\frac{N_0}{2}\right)^3 \left[\frac{f^2}{2} - 3Bf + \frac{9}{2}B^2\right] + M_5 \left(\frac{N_0}{2}\right)^5 \\ \quad \cdot \left[\frac{-f^4}{6} + \frac{5}{3}Bf^3 - 5B^2f^2 + \frac{5}{3}B^3f + \frac{55}{6}B^4\right] \\ \quad + M_7 \left(\frac{N_0}{2}\right)^7 \left[\frac{15}{720}f^6 - \frac{35}{120}Bf^5 + \frac{63}{48}B^2f^4 \right. \\ \qquad \left. - \frac{35}{36}B^3f^3 - \frac{273}{48}B^4f^2 \right. \\ \qquad \left. - \frac{35}{120}B^5f + \frac{23\,583}{720}B^6\right], \\ \qquad B < f < 3B. \end{cases} \tag{29}$$

Using PSD functions of the main amplifier and feedforward output, we can also find out the total power at the main and adjacent channels in closed form by integrating the above expressions over the specified bandwidths to yield

$$P_{\text{main}} = \frac{1}{2}\int_{-B}^{B} P_m(f)\,df = N_1 \frac{K}{2} + \frac{8}{3} N_3 \left(\frac{K}{2}\right)^3 \tag{30}$$

$$P_{\text{macp}} = \int_{B}^{3B} P_m(f)\,df = \frac{4}{3} N_3 \left(\frac{K}{2}\right)^3 \tag{31}$$

$$\begin{aligned} P_{\text{out}} &= \frac{1}{2}\int_{-B}^{B} P_y(f)\,df \\ &= M_1 \frac{K}{2} + \frac{8}{3} M_3 \left(\frac{K}{2}\right)^3 + \frac{44}{5} M_5 \left(\frac{K}{2}\right)^5 \end{aligned} \tag{32}$$

$$\begin{aligned} P_{\text{outacp}} &= \int_{B}^{3B} P_y(f)\,df \\ &= \frac{4}{3} M_3 \left(\frac{K}{2}\right)^3 + \frac{104}{15} M_5 \left(\frac{K}{2}\right)^5 + \frac{3176}{105} M_7 \left(\frac{K}{2}\right)^7 \end{aligned} \tag{33}$$

where

$P_{\text{main}}$ total power at the output of the main amplifier;
$P_{\text{macp}}$ total ACP at the output of the main amplifier;
$P_{\text{out}}$ total power at the output of the feedforward;
$P_{\text{outacp}}$ total ACP at the output of the feedforward.

## IV. Simulation and Verifications

In order to verify the expressions derived, we simulated the system using the HP ADS simulation program. The zero-mean band-limited white Gaussian noise input, which represents $n$-coded CDMA signals has been generated using the component palette additive white Gaussian channel (AWGC) which produces white Gaussian noise with a sampling period of 0.27 $\mu$s and duration of 2700 $\mu$s. This signal is then passed through a lowpass Chebyshev filter whose passband frequency is 615 kHz, to achieve band-limited white Gaussian noise. Note that a band-limited white Gaussian noise whose bandwidth is compatible to CDMA (1.23 MHz) has been used as the stimulus instead of real CDMA data because the essential point regarding this analysis is the nature of the source, and the analysis applies to any CDMA data as long as it obeys the Gaussian noise nature. Nonlinearities of the amplifiers used in HP ADS have been limited to the *output IP3* (third-order intercept) only. Power spectrum of the main amplifier and the feedforward output are simulated using fast Fourier transform (FFT) analyzers. The number of FFT points ($Npoints$) should be the power of 2; if not, the closest power of 2 is chosen. In our case, since the number of data points is 10 000, $Npoints$ is chosen as 8192. The resolution bandwidth (RBW) of the power spectrum is $1/(Npoints \times Ts)$ which is equal to 451.8 Hz [1/(8192 $\times$ 0.27 $\mu$s)] in our simulation. In order to decrease the RBW, time duration must be increased.

In order to achieve a better understanding of the signal processing and power spectrum analysis, we adapted the same feedforward system to the MATLAB environment. The time-domain envelope data at the output of the main amplifier, input of the error amplifier, and output of the feedforward are computed using (3)–(11). The power spectrums of these time-domain envelope data have been computed by MATLAB and compared with ADS results to verify the formulation of the feedforward system. Thus, our simulation has been intended to be flexible to any arbitrary time data input. In order to estimate the PSD for wide-sense stationary discrete time data, the following relation can be used [8]:

$$P_{xx}(f) = \frac{|X_N(f)|^2}{NT_s} \tag{34}$$

where $T_s$ is the sampling period (0.27 $\mu$s). In MATLAB simulation, we made use of the FFT function for the rapid computation of the discrete Fourier series. Hence, the PSD estimate has been computed using the following formula:

$$P_{xx}(f) = \frac{T_s^2 * |\text{FFT}(x,\, N)|^2}{(NT_s)} \tag{35}$$

where $N$ is chosen to be power of 2 (8192) closest to the number of data points, which is 10 000 in our case. Note that for a 50-$\Omega$ system the expression above must be divided by 50.

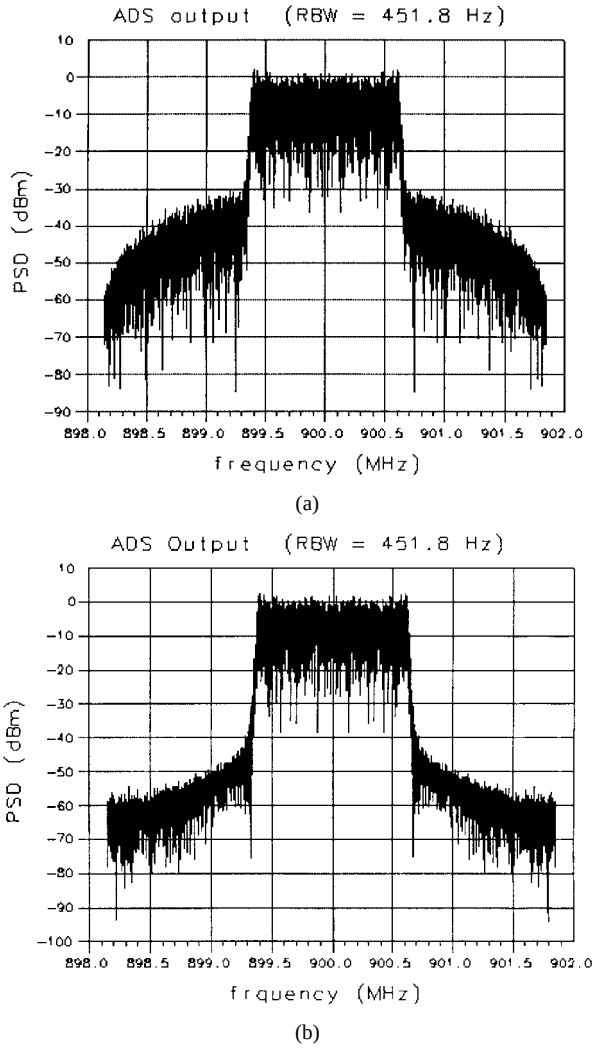


Fig. 3. (a) ADS simulation for main amplifier output. (b) ADS simulation for feedforward output ($C_1 = 10$ dB, $C_2 = 20$ dB, $C_3 = 10$ dB, $C_4 = 10$ dB, $Gm = 20$ dB, $\text{IP3}^m = 46$ dBm, $Ge = 40$ dB, and $\text{IP3}^e = 50$ dBm).

The results of ADS and MATLAB simulation of the power spectrum of the main amplifier and feedforward output are shown and compared in Figs. 3 and 4 for the given parameters ($C1 = 10$ dB, $C2 = 20$ dB, $C3 = 10$ dB, $C4 = 10$ dB, $Gm = 20$ dB, $\text{IP3}^m = 46$ dBm, $Ge = 40$ dB, and $\text{IP3}^e = 50$ dBm). Close observation of the figures shows that ADS and MATLAB simulation results agree with each other. It should be noted that MATLAB results are added by 26.5 dB ($10 \times \log 10(451.8$ Hz)) to be equivalent to ADS results. Both ADS and MATLAB results are around the 900-MHz carrier frequency. These results are a good validation for the expressions derived and used in the MATLAB simulation. Note that these expressions are also used for closed-form derivations.

## V. Verification of Closed-Form Expressions and Discussions

Since MATLAB simulations are verified with HP ADS results, the derived closed-form expressions can now be validated using the MATLAB environment which is a more convenient and faster simulation environment, and the input data can be processed so that its characteristic is similar to the one used

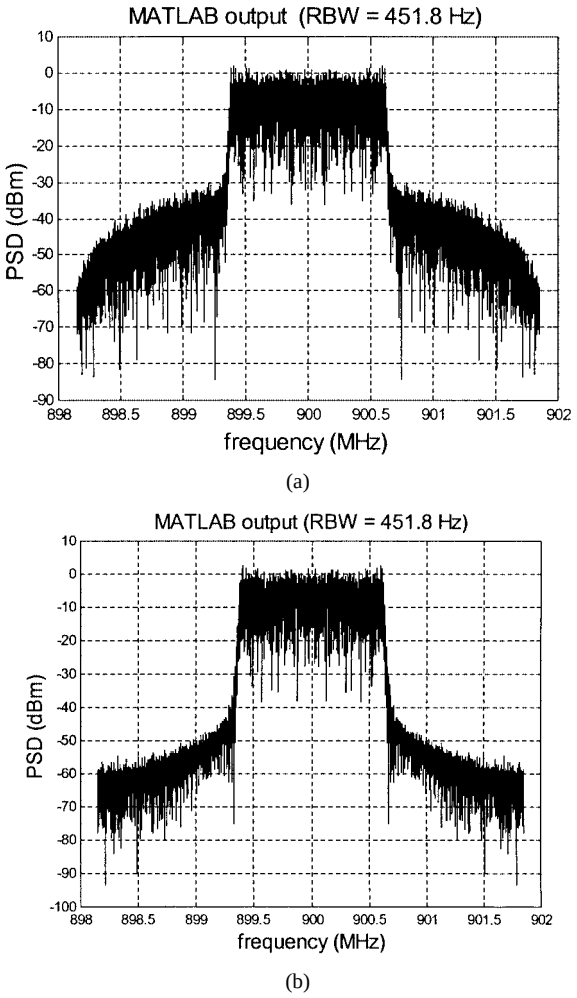


Fig. 4. (a) MATLAB simulation for main amplifier output. (b) ADS simulation for feedforward output ($C_1 = 10$ dB, $C_2 = 20$ dB, $C_3 = 10$ dB, $C_4 = 10$ dB, $Gm = 20$ dB, $\mathrm{IP3}^m = 46$ dBm, $Ge = 40$ dB, and $\mathrm{IP3}^e = 50$ dBm).

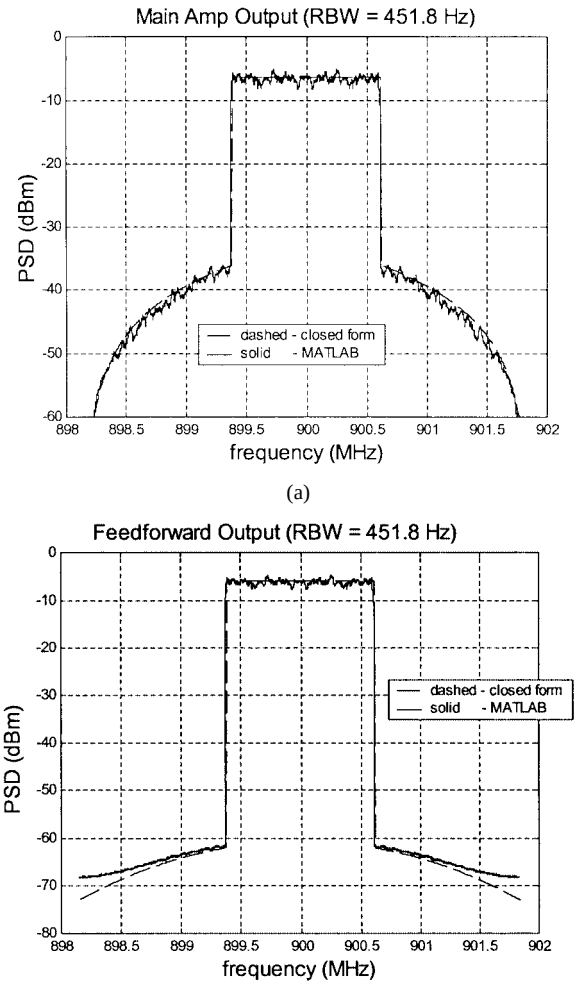


Fig. 5. Comparison of MATLAB simulation and closed-form expressions for (a) main amplifier output and (b) feedforward output ($C_1 = 10$ dB, $C_2 = 20$ dB, $C_3 = 10$ dB, $C_4 = 10$ dB, $Gm = 20$ dB, $\mathrm{IP3}^m = 46$ dBm, $Ge = 40$ dB, $\mathrm{IP3}^e = 50$ dBm, $P\mathrm{out} = 28.5$ dBm).

for the closed-form derivations. Since the input data used for closed-form expression are perfect band-limited white Gaussian noise with zero mean, the power spectrum is concentrated in the main channel and ACP does not exist. In order to create similar input data in the MATLAB environment, the adjacent channels of the generated ADS data have been filtered out ideally. The closed-form expressions and MATLAB simulations for the main amplifier and feedforward output are compared in Fig. 5 for $C_1 = 10$ dB, $C_2 = 20$ dB, $C_3 = 10$ dB, $C_4 = 10$ dB, $Gm = 20$ dB, $\mathrm{IP3}^m = 46$ dBm, $Ge = 40$ dB, $\mathrm{IP3}^e = 50$ dBm, and $P\mathrm{out} = 28.5$ dBm.

Note that closed-form results coincide with MATLAB simulations. The small deviations are possibly due to the techniques used for averaging MATLAB simulation results and deviation of the generated noise data from the ideal band-limited white Gaussian noise. After validating the closed-form expressions, we can use (30)–(33) in order to compute the main channel power and ACP of the main amplifier and feedforward outputs. For our case, these quantities are computed and compared with simulation results in Table I. Note that the main amplifier output power is approximately 0.5 dB lower than it should be because of the existence of in-band distortion. The amount of in-band distortion can be computed as 4.3 dBm using (30) and setting $E_1$ in (19) to zero. After the carrier cancellation, the error cancellation loop cancels the in-band distortion and the feedforward compensates for this loss. To show the utility of the closed-form results, a similar comparison has been made for different coupling values in Table II to take loop mismatches and losses into consideration.

TABLE I
QUANTITATIVE COMPARISON OF THE CLOSED-FORM AND SIMULATION RESULTS ($C_1 = 10$ dB, $C_2 = 20$ dB, $C_3 = 10$ dB, $C_4 = 10$ dB, $Gm = 20$ dB, $\mathrm{IP3}^m = 46$ dBm, $Ge = 40$ dB, $\mathrm{IP3}^e = 50$ dBm, $P\mathrm{out} = 28.5$ dBm)

| | Closed Form | Simulation |
|---|---|---|
| **Pmain (dBm)** | 28.0 | 28.0 |
| **Pmain-acp(dBm)** | -3.5 | -4.0 |
| **Pout (dBm)** | 28.5 | 28.5 |
| **Pout-acp (dBm)** | -28.1 | -27.2 |

Since the nonlinearities of the main and error amplifiers are limited by third-order power series expansion, there is a critical input voltage up to where the third-order model represents the nonlinearity correctly. As the input voltage increases, the output begins to compress and at the critical point the output is just at the saturation. In MATLAB simulation, the output is allowed

TABLE II
QUANTITATIVE COMPARISON OF THE CLOSED-FORM AND SIMULATION RESULTS FOR DIFFERENT LOOP MISMATCHES ($L_1 = L_2 = L_3 = L_4 = 0.3$ dB $C_1 = 10$ dB, $C_2 = 20$ dB, $C_3 = 10$ dB, $C_4 = 10$ dB, $Gm = 20$ dB, $\mathrm{IP3}^m = 46$ dBm, $Ge = 40$ dB, $\mathrm{IP3}^e = 50$ dBm, $P\mathrm{out} = 28.5$ dBm)

| | C1 = 9 dB | | C2 = 19 dB | | C4 = 9 dB | |
|---|---|---|---|---|---|---|
| | Closed Form | Simulation | Closed Form | Simulation | Closed Form | Simulation |
| **Pout(dBm)** | 28.7 | 28.7 | 26.5 | 26.5 | 27.7 | 27.7 |
| **Pout-acp(dBm)** | -23.8 | -22.5 | -19.1 | -19.7 | -19.8 | -20.7 |

to be constant at the saturation value beyond this critical point. However, for closed-form expressions, we cannot make a similar adjustment and beyond this critical point the output voltage value deviates from the saturation point which makes the results incorrect. The range of the input voltage value can be increased with the order of nonlinearities. As a consequence of this observation, it can be deduced that there exists a minimum IP3 for the main and error amplifiers where the closed-form expressions give compatible results with simulation. The critical input voltage value for the main and error amplifiers can be determined by differentiating the power series expansions (5) and (9) with respect to input voltage and equating them to zero. Hence we obtain

$$V_{\mathrm{si\_crit}} = \sqrt{\frac{-a_1}{3a_3 l_1^2}} \tag{36}$$

$$V_{\mathrm{se\_crit}} = \sqrt{\frac{-b_1}{3b_3}}. \tag{37}$$

If the maximum input voltage value to the system is known, then the minimum IP3 value of the main amplifier, with which closed-form expressions can be used for a 50-$\Omega$ system, can be calculated using (3), (6), and (36) to obtain

$$\mathrm{IP}_3^m = G_m + 20\log(V_{\mathrm{si\_max}}) + 20\log l_1 + 14.77 \tag{38}$$

noting that $V_{\mathrm{si\_max}}$ is the absolute maximum voltage level at the input of the main amplifier and now is the critical voltage $V_{\mathrm{si\_crit}}$ for the worst case. Absolute maximum voltage level at the input of the error amplifier ($V_{\mathrm{se\_max}}$) and the required minimum IP3 can be computed using the following equations:

$$V_{\mathrm{se\_max}} = \left| V_{\mathrm{si\_max}} \left( \frac{a_1 l_1}{C_2 C_3} - \frac{l_3}{C_1} \right) + V_{\mathrm{si\_max}}^3 \left( \frac{a_3 l_1^3}{C_2 C_3} \right) \right| \tag{39}$$

$$\mathrm{IP}_3^e = G_e + 20\log(V_{\mathrm{se\_max}}) + 14.77. \tag{40}$$

In our case, time-domain data of the main amplifier and error amplifier inputs are seen in Fig. 6. Note that the absolute maximum voltage value at the main amplifier input is 3.55 V. Hence, using (38), the minimum required IP3 for the main amplifier can be computed as 45.8 dBm. For this main amplifier IP3, the absolute maximum at the input of the error amplifier is computed as 0.37 V using (39), which can also be verified in Fig. 6. Finally, by using (40), the minimum required error amplifier IP3 is found as 46.2 dBm. These values are the minimum required IP3 parameters for the coincidence of the simulation and closed-form results.

The envelope peak-to-average ratio of the main amplifier input is approximately 13 dB. The envelope peak-to-average ratio for the error amplifier input increases up to 26 dB. The

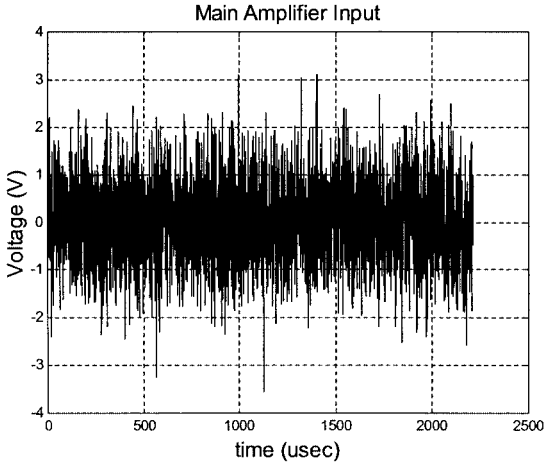


(a)

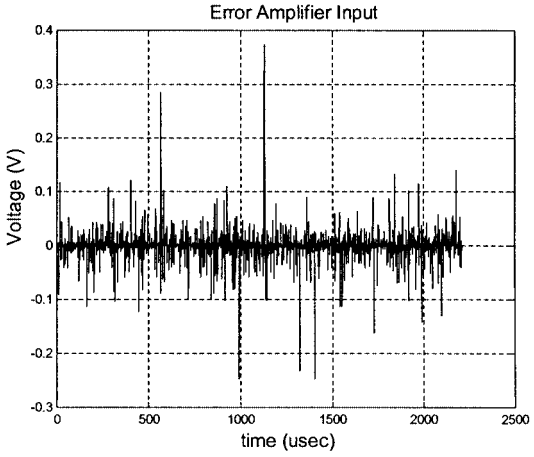


(b)

Fig. 6. (a) Time-domain data at the input of the main amplifier for $\mathrm{IP3}^m = 45.8$ dBm. (b) Time-domain data at the input of the error amplifier for $\mathrm{IP3}^m = 45.8$ dBm.

average power at the input of the error amplifier can be computed as $-25.5$ dBm. Hence, the average power at the output of the 40-dB gain error amplifier is approximately 14.5 dBm. Considering the crest factor and 10 dB extra for IP3, we end up with at least 50.5 dBm for IP3 of the error amplifier. Although the required average power at the output of the error amplifier is not that high, because of the high peak-to-average ratio at the input of the error amplifier, IP3 of the amplifier needs to be quite high to not introduce additional distortion products. Unfortunately, among other factors, this requirement makes the feedforward technique inefficient. However, efficiency can be optimized by careful adjustment of the parameters for the best amplitude matching within the loops, for the minimum peak-to-average ratio and average power at the input of the

error amplifier [9]–[12]. The derived closed-form expressions are believed to be a convenient and fast tool to make these tradeoffs for a given output linearity.

For the lossless case where perfect matching within the loops exists, the coefficients $D_3$, $D_5$, and $D_7$ in (12) tend to vanish and the expression derived for the ACP of the feedforward output (33) reduces to the following:

$$P_{\text{outacp}} = 6\,846\,120 D_9^2 K^9. \tag{41}$$

If we substitute the expression for $D_9$ and (27) into the above expression, we obtain

$$P_{\text{outacp}} = 6\,846\,120\,\frac{b_5^2 a_3^6}{C_2^6 C_3^6 C_4^2}\,\frac{2^9 P_m^9}{a_1^{18}}. \tag{42}$$

By making use of (3), (6), and (10), (42) can be reduced to the following compact relationship:

$$\text{IP}_3^e + 3\text{IP}_3^m = 35.68 + \frac{9}{2}P_m - \frac{1}{2}P_{\text{outacp}} + C_4. \tag{43}$$

Hence, (43) relates the desired output ACP to the nonlinearities of the main and error amplifiers, the proposed output power, and the coupling coefficient of C4 for a lossless feedforward circuit with perfect matching. This relationship is verified in our example ($\text{IP}_3^e = 50$ dBm, $\text{IP}_3^m = 46$ dBm, $P_m = 28.5$ dBm, $P_{\text{outacp}} = -28.1$ dBm, and $C_4 = 10$ dB). For a fixed output power, ACP and C4, third-order nonlinearities of the main and error amplifiers can be adjusted for optimum overall efficiency.

The analysis explained so far assumes that there is no delay mismatch. Addition of the delay mismatches, especially the one in the first loop, would make the closed-form formulations very complex even though the model is based upon third-order nonlinearities. However, to show the effect of delay mismatches to the formulations, assuming there is no phase mismatch in the carrier, we modified the formulations for the delay mismatch in the second loop $\tau_2$, which is relatively simple to analyze. Taking $\tau_2$ into consideration modifies (12) into the following:

$$\begin{aligned} y(t) = {} & D_1' s_i(t) + D_3' s_i^3(t) + D_5' s_i^5(t) + D_7' s_i^7(t) + D_9' s_i^9(t) \\ & + D_1'' s_i(t-\tau_2) + D_3'' s_i^3(t-\tau_2) \end{aligned} \tag{44}$$

where coefficients can be found in Appendix C. After taking the AF of (44), we obtain a modified form of (23) as

$$\begin{aligned} R_y(\tau) = {} & E\{y(t)y(t+\tau)\} \\ = {} & M_1' R_{si}(\tau) + M_3' R_{si}^3(\tau) + M_5' R_{si}^5(\tau) + M_7' R_{si}^7(\tau) \\ & + M_9' R_{si}^9(\tau) + M_1''[R_{si}(\tau-\tau_2) + R_{si}(\tau+\tau_2)] \\ & + M_3''[R_{si}^3(\tau-\tau_2) + R_{si}^3(\tau+\tau_2)] \end{aligned} \tag{45}$$

where coefficients can be found in Appendix D. The PSD at the output of the feedforward can be computed by taking the Fourier transform of (45) to yield

$$\begin{aligned} P_y(f) = {} & [M_1' + 2M_1'' \cos(2\pi f \tau_2)] P_s(f) \\ & + [M_3' + 2M_3'' \cos(2\pi f \tau_2)] P_s(f) \otimes P_s(f) \otimes P_s(f) \\ & + M_5' P_s(f) \otimes P_s(f) \otimes P_s(f) \otimes P_s(f) \otimes P_s(f) \\ & + M_7' P_s(f) \otimes \cdots \otimes P_s(f). \end{aligned} \tag{46}$$

The PSD expression for the feedforward output is similar to the one in (29), except that $M_1$, $M_3$, $M_5$, and $M_7$ are replaced with $[M_1' + 2M_1'' \cos(2\pi f \tau_2)]$, $[M_3' + 2M_3'' \cos(2\pi f \tau_2)]$, $M_5'$, and $M_7'$, respectively. Expressions for the total power at the main and adjacent channels are also given as (47) and (48), shown at the bottom of the following page, where $A = \pi B \tau_2$. Graphical and quantitative comparisons of the closed-form formulations and simulation results for $\tau_2 = 270$ ns are shown in Fig. 7 and Table III, respectively. Note that the results are quite close to each other. A comparison of Tables I and III emphasizes the drastic effect of delay mismatch on the linearization performance of the system.

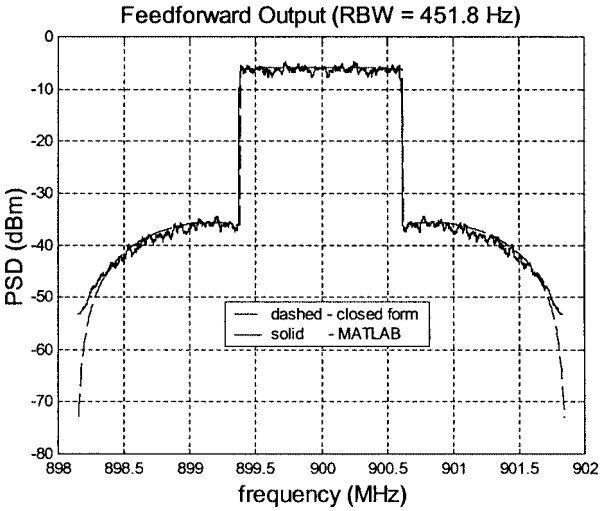


Fig. 7. Comparison of MATLAB simulation and closed-form expressions for feedforward output ($C_1 = 10$ dB, $C_2 = 20$ dB, $C_3 = 10$ dB, $C_4 = 10$ dB, $Gm = 20$ dB, $\text{IP3}^m = 46$ dBm, $Ge = 40$ dB, $\text{IP3}^e = 50$ dBm, $P\text{out} = 28.5$ dBm, $\tau_2 = 270$ ns).

TABLE III
QUANTITATIVE COMPARISON OF THE CLOSED-FORM AND SIMULATION RESULTS FOR $\tau_2 = 270$ ns ($C_1 = 10$ dB, $C_2 = 20$ dB, $C_3 = 10$ dB, $C_4 = 10$ dB, $Gm = 20$ dB, $\text{IP3}^m = 46$ dBm, $Ge = 40$ dB, $\text{IP3}^e = 50$ dBm, AND $P\text{out} = 28.5$ dBm)

| | Closed Form | Simulation |
|---|---|---|
| **Pout (dBm)** | 28.4 | 28.4 |
| **Pout-acp (dBm)** | 0.1 | -1.1 |

TABLE IV
MAIN AMPLIFIER AND FEEDFORWARD OUTPUTS FOR VARIOUS FIFTH-ORDER NONLINEARITIES—$a_5$ VALUES ($C_1 = 10$ dB, $C_2 = 20$ dB, $C_3 = 10$ dB, $C_4 = 10$ dB, $Gm = 20$ dB, $\text{IP3}^m = 46$ dBm, $Ge = 40$ dB, $\text{IP3}^e = 50$ dBm, AND $P\text{out} = 28.5$ dBm)

| IP5 (dBm) | $a_5$ | Pmain (dBm) | Pmain-acp (dBm) | Pout (dBm) | Pout-acp (dBm) |
|---|---|---|---|---|---|
| 70 | -1e-7 | 28.0 | -4.0 | 28.5 | -27.2 |
| 60 | -1e-5 | 28.0 | -4.0 | 28.5 | -27.2 |
| 50 | -0.001 | 28.0 | -3.75 | 28.5 | -26.0 |
| 48 | -0.0025 | 28.0 | -3.4 | 28.5 | -24.4 |
| 46 | -0.006 | 28.0 | -2.5 | 28.5 | -21.7 |
| 44 | -0.016 | 27.97 | -1.0 | 28.5 | -17.9 |
| 42 | -0.040 | 27.8 | 1.2 | 28.47 | -13.8 |

In our model, the main and error amplifiers are based on third-order nonlinearities only. Equations that have been derived and the analysis show that even third-order approximations lead to tedious and complex closed-form expressions for the whole system since the system involves two nonlinear amplifiers together. Table IV demonstrates the effect of additional fifth-order

TABLE V
EQUIVALENT THIRD-ORDER MODEL $a_3$ COEFFICIENTS AND IP3$^m$ VALUES FOR THE FIFTH-ORDER NONLINEARITIES PRESENTED IN TABLE IV ($C_1 = 10$ dB, $C_2 = 20$ dB, $C_3 = 10$ dB, $C_4 = 10$ dB, $Gm = 20$ dB, $Ge = 40$ dB, IP3$^e = 50$ dBm, AND $P\text{out} = 28.5$ dBm)

| IP3 (dBm) | $a_3$ | Pmain (dBm) | Pmain-acp (dBm) | Pout (dBm) | Pout-acp (dBm) |
|---|---|---|---|---|---|
| 46 | -0.25 | 28.0 | -4.0 | 28.5 | -27.2 |
| 46 | -0.25 | 28.0 | -4.0 | 28.5 | -27.2 |
| 45.8 | -0.263 | 28.0 | -3.65 | 28.5 | -26.0 |
| 45.7 | -0.269 | 28.0 | -3.4 | 28.5 | -25.4 |
| 45.2 | -0.302 | 27.97 | -2.4 | 28.5 | -22.6 |
| 44.4 | -0.363 | 27.86 | -0.9 | 28.5 | -18.7 |
| 43.2 | -0.479 | 27.66 | 1.25 | 28.47 | -14.1 |

nonlinearity for the main amplifier on the output distortion products of the main amplifier and the feedforward system. Hence, (5) expands to the following form:

$$s_m(t) = l_1 a_1 s_i(t) + l_1^3 a_3 s_i^3(t) + l_1^5 a_5 s_i^5(t). \tag{49}$$

Note that for our example ($G_m = 20$ dB, IP3$^m = 46$ dBm) $a_1 = 10$ and $a_3 = -0.25$. For $a_5 < -0.002$ which corresponds to the case IP5 $< 48$ dBm, the simulation results begin to deviate from the third-order model. However, Table V shows that there exists an approximately equivalent third-order model for the main amplifier that would fit the fifth-order one to give similar quantities of distortion products at the output of the main amplifier and the feedforward system. Table V demonstrates the equivalent $a_3$ values for various fifth-order nonlinearities in Table IV. A comparison of these two tables shows that distortion products at the output are closed to each other within 1 dB.

## VI. CONCLUSION

In this paper, we derived a closed-form expression to be used to compute the output main channel and ACP of a simple feedforward circuit for CDMA applications. Eventually we ended up with a formulation which relates the output PSD to circuit parameters. This formulation provides a tool to control the circuit parameters for optimum efficiency and linearity. In order to validate our formulations, the same system has been simulated in HP ADS with its own built-in components and generated band-limited white Gaussian noise data. In order to understand the signal processing and the power spectrum analysis and to verify some of the formulations used to derive the closed-form expressions, we adapted the same system to MATLAB and we found a correct formulation, which makes the ADS and MATLAB results identical. The computed power spectral densities of the main channel and adjacent channel at the output of the main amplifier and feedforward circuit using the derived closed-form expressions are in good agreement with the MATLAB simulation results.

The input signal used in closed-form formulations is an ideal band-limited zero mean white Gaussian noise which has an inherent envelope peak-to-average ratio (12–13 dB). Since the nonlinearities of the main and error amplifiers are represented by their third-order intercept point (IP3) only, we found out that there is a minimum IP3 where closed-form formulations agree with practical simulations, and it has been shown that this critical IP3 value and thus the range of validity can be calculated in terms of maximum input voltage applied to the feedforward system.

For the case where the carrier and error cancellation loops are balanced and the system is lossless, we ended up with a useful formulation that relates the desired ACP and output power to the IP3s of the main and error amplifiers. This formulation gives us a chance to trade off size, linearity, and efficiency against each other.

Finally, we included delay mismatch in the second loop to the analysis and modified the closed-form expressions accordingly. Since it yields lengthy expressions, delay mismatch in the first loop has not been included in this paper.

This analysis can be extended to a more realistic case where the amplifiers are modeled by their fifth-order nonlinearities. However, the calculations become very tedious because one will have to face with 25th-order convolutions and functions rather than ninth-order. Nevertheless, comparison of simulations for the two cases, i.e., third- and fifth-order amplifier models, is presented to have an idea about the practical use of the third-order model.

## APPENDIX A

Expressions for the coefficients indicated in (12) are listed as follows:

$$D_1 = l_1 l_2 l_4 a_1 + \frac{b_1 l_3}{C_1 C_4} - \frac{a_1 b_1 l_1}{C_2 C_3 C_4}$$

$$P_{\text{out}} = \frac{N_0}{2}\frac{[M_1' A + M_1'' \sin(2A)]}{\pi\tau_2} + \left(\frac{N_0}{2}\right)^3 \frac{[16M_3' A^3 - 6M_3'' A\cos(2A) + 12M_3'' A^2 \sin(2A) + 3M_3'' \sin(2A)]}{6(\pi\tau_2)^3} + \frac{44}{5} M_5 \left(\frac{K}{2}\right)^5 \tag{47}$$

$$P_{\text{outacp}} = \left(\frac{N_0}{2}\right)^3 \frac{[16M_3' A^3 + 12M_3'' A\cos(2A) + (3 - 24A^2)M_3\text{"} \sin(2A) - 3M_3'' \sin(6A)]}{12(\pi\tau_2)^3} + \frac{104}{15} M_5' \left(\frac{K}{2}\right)^5 + \frac{3176}{105} M_7' \left(\frac{K}{2}\right)^7 \tag{48}$$

$$D_3 = l_1^3 l_2 l_4 a_3 - \frac{a_3 b_1 l_1^3}{C_2 C_3 C_4} + \frac{b_3 l_3^3}{C_1^3 C_4} - \frac{3 b_3 a_1 l_1 l_3^2}{C_1^2 C_2 C_3 C_4} + \frac{3 a_1^2 b_3 l_1^2 l_3}{C_1 C_4 C_2^2 C_3^2} - \frac{a_1^3 b_3 l_1^3}{C_4 C_2^3 C_3^3}$$

$$D_5 = \frac{-3 b_3 a_3 l_3^2 l_1^3}{C_1^2 C_2 C_3 C_4} + \frac{6 a_1 a_3 b_3 l_1^4 l_3}{C_1 C_2^2 C_3^2 C_4} - \frac{3 a_1^2 a_3 b_3 l_1^5}{C_2^3 C_3^3 C_4}$$

$$D_7 = \frac{3 a_3^2 b_3 l_3 l_1^6}{C_1 C_2^2 C_3^2 C_4} - \frac{3 a_1 a_3^2 b_3 l_1^7}{C_2^3 C_3^3 C_4}$$

$$D_9 = \frac{-b_3 a_3^3 l_1^9}{C_2^3 C_3^3 C_4}.$$

## Appendix B

Coefficients indicated in (23) are computed using (24) and listed as follows:

$$\begin{aligned} M_1 &= D_1^2 + 6 D_1 D_3 K + 30 D_1 D_5 K^2 + 9 D_3^2 K^2 \\ &\quad + 90 D_3 D_5 K^3 + 225 D_5^2 K^4 + 210 D_1 D_7 K^3 \\ &\quad + 1890 D_1 D_9 K^4 + 630 D_3 D_7 K^4 + 5670 D_3 D_9 K^5 \\ &\quad + 3150 D_5 D_7 K^5 + 28\,350 D_5 D_9 K^6 + 11\,025 D_7^2 K^6 \\ &\quad + 198\,450 D_7 D_9 K^7 + 893\,025 D_9^2 K^8 \end{aligned}$$

$$\begin{aligned} M_3 &= 6 D_3^2 + 120 D_3 D_5 K + 600 D_5^2 K^2 + 1260 D_3 D_7 K^2 \\ &\quad + 15\,120 D_3 D_9 K^3 + 12\,600 D_5 D_7 K^3 \\ &\quad + 151\,200 D_5 D_9 K^4 + 66\,150 D_7^2 K^4 \\ &\quad + 1\,587\,600 D_7 D_9 K^5 + 9\,525\,600 D_9^2 K^6 \end{aligned}$$

$$\begin{aligned} M_5 &= 120 D_5^2 + 5040 D_5 D_7 K + 90\,720 D_5 D_9 K^2 \\ &\quad + 52\,920 D_7^2 K^2 + 1\,905\,120 D_7 D_9 K^3 \\ &\quad + 17\,146\,080 D_9^2 K^4 \end{aligned}$$

$$M_7 = 5040 D_7^2 + 362\,880 D_7 D_9 K + 6\,531\,840 D_9^2 K^2$$

$$M_9 = 362\,880 D_9^2.$$

## Appendix C

Expressions for the coefficients indicated in (44) are listed as follows:

$$D_1'' = l_1 l_2 l_4 a_1$$

$$D_3'' = l_1^3 l_2 l_4 a_3$$

$$D_1' = D_1 - D_1''$$

$$D_3' = D_3 - D_3''$$

$$D_5' = D_5$$

$$D_7' = D_7$$

$$D_9' = D_9.$$

## Appendix D

Coefficients indicated in (45) are listed as follows:

$$\begin{aligned} M_1' &= D_1'^2 + 6 D_1' D_3' K + 30 D_1' D_5' K^2 + 9 D_3'^2 K^2 \\ &\quad + 90 D_3' D_5' K^3 + 225 D_5'^2 K^4 + 210 D_1' D_7' K^3 \\ &\quad + 1890 D_1' D_9' K^4 + 630 D_3' D_7' K^4 + 5670 D_3' D_9' K^5 \\ &\quad + 3150 D_5' D_7' K^5 + 28\,350 D_5' D_9' K^6 + 11\,025 D_7'^2 K^6 \\ &\quad + 198\,450 D_7' D_9' K^7 + 893\,025 D_9'^2 K^8 + D_1''^2 \\ &\quad + 9 D_3''^2 K^2 + 6 D_1'' D_3'' K \end{aligned}$$

$$\begin{aligned} M_3' &= 6 D_3'^2 + 120 D_3' D_5' K + 600 D_5'^2 K^2 + 1260 D_3' D_7' K^2 \\ &\quad + 15\,120 D_3' D_9' K^3 + 12\,600 D_5' D_7' K^3 \\ &\quad + 151\,200 D_5' D_9' K^4 + 66\,150 D_7'^2 K^4 \\ &\quad + 1\,587\,600 D_7' D_9' K^5 + 9\,525\,600 D_9'^2 K^6 + 6 D_3''^2 \end{aligned}$$

$$\begin{aligned} M_1'' &= 945 D_9' D_1'' K^4 + 2835 D_9' D_3'' K^5 + 105 D_7' D_1'' K^3 \\ &\quad + 315 D_7' D_3'' K^4 + 15 D_5' D_1'' K^2 + 45 D_5' D_3'' K^3 \\ &\quad + 3 D_3' D_1'' K + 9 D_3' D_3'' K^2 + D_1' D_1'' + 3 D_1' D_3'' K \end{aligned}$$

$$M_3'' = 7560 D_9' D_3'' K^3 + 630 D_7' D_3'' K^2 + 60 D_5' D_3'' K + 6 D_3' D_3''$$

$$M_5' = M_5$$

$$M_7' = M_7$$

$$M_9' = M_9.$$

## Acknowledgment

The authors would like to thank Dr. M. Eron, Ericsson Amplifier Technologies Inc., NY, for his valuable suggestions and discussions throughout the work.

## References

[1] P. K. Kenington, "Linearized RF transmitter techniques," presented at the IEEE MTT-S Workshop, Baltimore, MD, June 1998.
[2] ——, "Linearization in base-station equipment," presented at the IEEE MTT-S Workshop, Boston, MA, June 2000.
[3] N. Pothecary, *Feedforward Linear Power Amplifiers*. Boston, MA: Artech House, 1999, pp. 125–140.
[4] Q. Wu, H. Xiao, and F. Li, "Linear RF power amplifier design for CDMA signals: A spectrum analysis approach," *Microwave J.*, pp. 22–40, Dec. 1998.
[5] T. T. Ha, *Solid-State Microwave Amplifier Design*. New York: Wiley, 1981, pp. 205–209.
[6] T. Wang and T. Brazil, "The estimation of volterra transfer functions with applications to RF power amplifier behavior evaluation for CDMA digital communications," in *IEEE MTT-S Int. Microwave Symp. Dig.*, 2000, pp. 425–428.
[7] S. Haykin, *Communication Systems*. New York: Wiley, 1983, pp. 277–279.
[8] M. Jeruchim, P. Balaban, and K. Shanmugan, *Simulation of Communication Systems*. New York: Plenum, 1994, pp. 533–539.
[9] E. E. Eid, F. M. Ghannouchi, and F. Beauregard, "Optimal feedforward linearization system design," *Microwave J.*, pp. 78–86, Nov. 1995.
[10] P. B. Kenington, "Efficiency of feedforward amplifiers," *Proc. Inst. Elect. Eng.*, pt. G, vol. 139, no. 5, pp. 591–593, Oct. 1992.
[11] R. J. Wilkinson and P. B. Kenington, "Specification of error amplifiers for use in feedforward transmitters," *Proc. Inst. Elect. Eng.*, pt. G, vol. 139, no. 4, pp. 477–480, Aug. 1992.
[12] K. J. Parsons and P. B. Kenington, "The efficiency of a feedforward amplifier with delay loss," *IEEE Trans. Veh. Technol.*, vol. 43, pp. 407–412, May 1994.

**A. Hakan Coskun** (S'92) was born in Ankara, Turkey, in 1972. He received the B.Sc. degree (with high honors) in electrical engineering from the Middle East Technical University (METU), Ankara, Turkey, in 1993, the M.Sc. degree in electrical engineering from Arizona State University, Tempe, in 1996, and is currently working toward the Ph.D. degree in electrical engineering at METU.

From 1993 to 1994, he was with Turkish Scientific and Technical Research Institute (TUBITAK), Ankara, Turkey, where he was involved with modeling of inertial navigation systems. Since 1996, he has been with ASELSAN Electronics Industries Inc., Ankara, Turkey, where he is a Senior Engineer responsible for the design and development of RF wide-band high-power amplifiers for wireless products. His current research interests are in the areas of power amplifier design and power amplifier linearization for wireless applications.

Mr. Coskun was the recipient of a Fulbright scholarship.

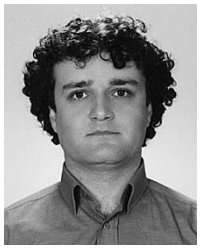

**Simsek Demir** (S'91–M'02) received the Ph.D. degree in electrical engineering from the Middle East Technical University (METU), Ankara, Turkey, in 1998.

He is currently an Assistant Professor with the Department of Electrical and Electronics Engineering, METU. In 1995, he was involved with linear MMIC amplifier research at the University of Massachusetts. In 1999, he was with IRCTR, Technical University of Delft, Delft, The Netherlands, where he contributed to the beam-forming network of the TARA system. His current interests are MMIC and RF MEMS applications, power amplifier linearization, beam-forming network design, and sparse antenna arrays.

Dr. Demir was the recipient of the NATO A2 Fellowship.